G.N. Kozhemyakin[1], S.Ya. Skipidarov[2], Yu.M. Krutov[1], A.N. Paraschenko[1], O.N. Ivanov[3], O.N. Soklakova[3]

[1]V. Dahl East-Ukrainian National University, 20 A, Molodyozhny kvartal, Lugansk, 91034, Ukraine;
[2]Closed JSC "SKTB "NORD", Ferrotec Corp., 3, Peschanyi kar'er, Moscow, 109383, Russia;
[3]Belgorod State University, 85, Pobedy Str., Belgorod, 308015, Russia

NANOSTRUCTURED BISMUTH AND ANTIMONY TELLURIDES FOR THERMOELECTRIC HEAT PUMP

The microstructure of p- and n-type bismuth and antimony telluride solid solutions prepared by hot extrusion was investigated. It was shown that the ingots of extruded thermoelectric materials consisted of nanocrystals as big as 8 to 30 nm. The thermoelectric parameters of extruded nanomaterials were measured and microstructure effect on their value was considered. These nanomaterials were used to produce p- and n-type legs to manufacture thermoelectric modules. The efficiency of thermoelectric modules operating as thermoelectric heat pumps in the temperature range of +10 to +45 °C was investigated. Two methods were developed for the measurement of conversion factor of thermoelectric modules. Maximum value of conversion factor reached 6.8 to 8.2 for heat transfer by thermoelectric module at electric power consumption 0.75 W. Electric power increase to 40 W contributed to reduction of conversion factor of thermoelectric modules to 1.8.
Key words: thermoelectricity; bismuth and antimony tellurides; nanocrystals; heat pump; conversion factor; heat transfer.

Introduction

Heat pumps are known to be more efficient than electric heating elements for heating in the temperature range of +10 °C to +40 °C [1]. For space heating at these temperatures heat pumps should possess high efficiency. Typical air heat pumps have conversion factor 3 – 4 when used for space heating in mild climate. However, with ambient temperature reduction to –18 °C the efficiency of heat pump is reduced to 1.0. Evaporative compression refrigeration devices can be used for heat pumps of geothermal systems. Such heat pumps have moving parts, limited service life and create noises. Moreover, for their operation environmentally hazardous coolants are employed.

Thermoelectric heat pumps also can have high conversion factor under special conditions, but without the above drawbacks [2-5]. For commercial use as a heater, conversion factor of thermoelectric heat pump should be more than 5 in the range of room temperatures. Energy conversion efficiency depends on the value of thermoelectric figure of merit $ZT = S^2\sigma T/k$, where Z is figure of merit, S is thermoEMF, σ is electric conductivity, T is absolute temperature and k is thermal conductivity. According to recent results of research [6, 7, 8] on the nanostructured crystalline ingots of p-type $Bi_xSb_{2-x}Te_3$, owing to thermal conductivity reduction the value of ZT has increased from 1.0 to 1.2 at room temperature. On the other hand, ZT for n-type $Bi_2Te_{3-x}Se_x$ has a low value about 0.85, which reduces the device efficiency. The results of this research showed a promising way for increasing the figure of merit ZT of thermoelectric materials and the efficiency of thermoelectric devices. It should be noted that incomplete information in the scientific literature on thermoelectric

heat pumps does not determine clearly enough the prospects of their use for heating systems.

The purpose of this work is to study structural perfection of extruded samples of solid solutions of bismuth and antimony chalcogenides, the effect of structure on the thermoelectric properties and conversion factor in the region of room temperatures. In this paper we present new results of research on the microstructure, thermoelectric properties and conversion factor of thermoelectric modules based on nanostructured *p*- and *n*-type legs that can be employed as heaters in the temperature range of +17 to +45 °C.

1. Experimental procedure

Thermoelement legs were manufactured by extrusion method. Bismuth, antimony, tellurium and selenium of 99.99 % purity were melted and crystallized prior to extrusion in the form of *p*-type $(Bi_2Te_3)_x$-$(Sb_2Te_3)_{1-x}$ ($x \approx 0.26$ mol.%) and *n*-type $(Bi_2Se_3)_x$-$(Bi_2Te_3)_{1-x}$ ($x \approx 0.06$ mol.%) ingots. Hot extrusion method was used to produce ingots of these solid solutions of diameter 30 mm according to the technology of SKTB "Nord". Samples in the form of discs 2 mm thick were cut from the ingots perpendicular to ingot axis direction to study their microstructure. The surfaces of discs were ground and polished with abrasive Al_2O_3 having grain size from 200 μm to 40 μm, respectively. After washing in distilled water the samples were etched in 50 % HNO_3 at a temperature about 50 °C for 10 to 15 minutes.

Microcrystals typical of polycrystals were not discovered under optical microscope on the prepared surface of samples of *p*- and *n*-type extruded thermoelectric materials. Therefore, the morphology of samples microstructure was studied under scanning electronic microscope (SEM "Quanta-600 H"). Samples for the measurement of thermoEMF, electric resistivity, thermal conductivity and carrier concentration were cut from ingots shaped as parallelepipeds of size $3 \times 4 \times 23$ mm^3 with their larger face oriented parallel and perpendicular to ingot axis. On their larger lateral face in depressions of diameter 0.3 mm and depth 0.4 mm iron-constantan thermocouples were secured whose wire diameter was about 100 μm.

The extruded *p*- and *n*-type ingots of diameter 30 mm were cut into thermoelement legs of size $1.6 \times 1.6 \times 1.6$ mm^3 of which thermoelectric modules of series TM-127-1.4-6.0 with the overall dimensions $40 \times 40 \times 3.8$ mm^3 were manufactured in SKTB "Nord".

The efficiency of heat transfer by these thermoelectric modules was studied. Conversion factor was measured by two methods under near-adiabatic conditions. Schematic of measurement by the first method using two copper plates is presented in Fig. 1. Heat input and transfer took place through the cold and hot heat spreaders of size $40 \times 40 \times 0.7$ mm^3 that are contact surfaces of thermoelectric modules. Heat flux passing through the module was measured through use of two copper plates of size $40 \times 40 \times 10$ mm^3.

The two surfaces of each copper plate were pre-polished with abrasive Al_2O_3 of size 40 μm. *BeO* paste was deposited to assure a reliable thermal contact between ceramic heat spreaders of thermoelectric modules and the surfaces of copper plates. The temperature of copper plates was measured by chromel-alumel thermocouples with the wire diameter 0.5 mm that were secured in the openings of diameter 1.0 mm and depth 1.5 mm on their lateral surfaces. A copper heat sink with running cold water was secured under the lower surface of cooled copper plate. The temperature of the hot upper copper plate was held constant during the experiment due to cooled copper heat sink. The thermoelectric modules and copper plates were thermally insulated with mineral wool. Such device design provided measurement of maximum temperature difference on thermoelectric modules with electric power requirement up to 45 W.

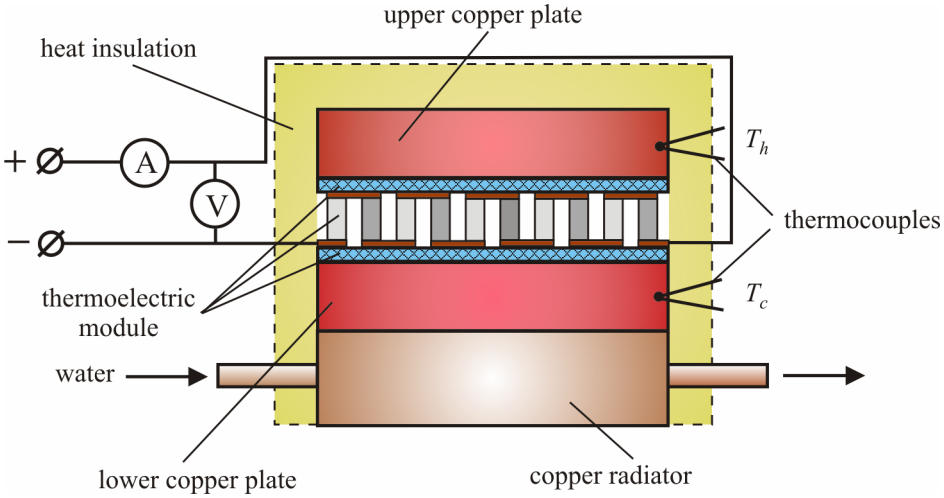

Fig. 1. Schematic of a device for conversion factor measurement by the method using two copper plates.

The second method of conversion factor measurement determined transfer of thermoelectric module heat from the electric heater to the copper plate. A device presented in Fig. 2 was developed for the second method. A thermoelectric module was secured on the electric heater of area 40×40 mm^2 and 2 mm thick. The lower surface of the electric heater rested on a base made of material with low thermal conductivity. One copper plate of size $40 \times 40 \times 10$ mm^3 and mass 174 g was used for heat flux measurement. This copper plate was secured on the upper heat spreader of thermoelectric module as an absorber of heat transferred to this module. A reliable thermal contact between the upper heat spreader of thermoelectric module and the copper plate was realized by means of *BeO* paste. The copper plate temperature was measured by copper-constantan thermocouple with the wire diameter 0.1 mm placed into opening of diameter 0.3 mm and depth 1 mm on the lateral surface of this plate. The air space between the copper plate, thermoelectric module, electric heater and metal case was filled with mineral wool for thermal insulation. Thermal flows from the five surfaces of the copper plate and thermoelectric module were compensated by two external heaters (lateral and upper). Temperature equality between the copper plate surfaces and the metal case walls was controlled by copper-constantan differential thermocouples. The conversion factor was measured 15 to 20 s after the thermoelectric module was switched on.

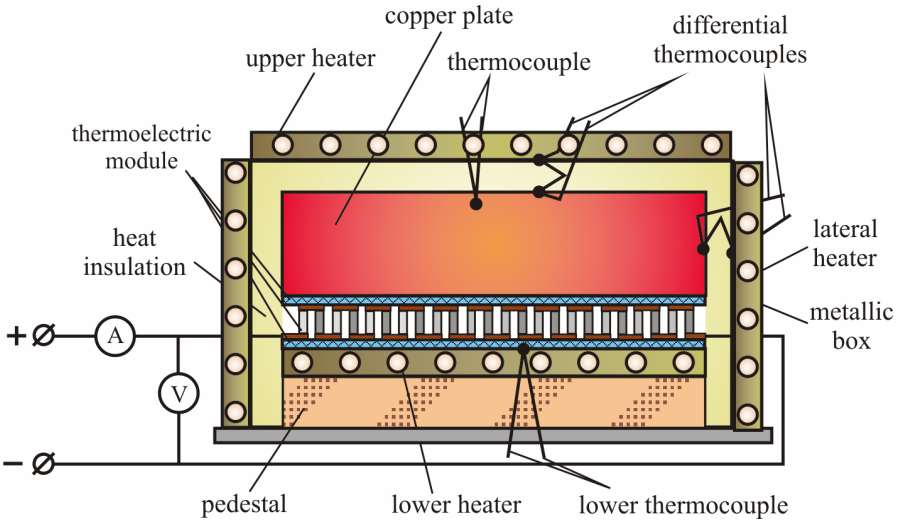

Fig. 2. Schematic of a device for conversion factor measurement by the method using a copper plate and a heater.

2. Structure of materials and their thermoelectric properties

Fig. 3 shows the pictures of structure morphology of *p*-type samples obtained by means of scanning electron microscope.

In *p*-type samples with a small magnification 40000× there were uniformly distributed crystallites and pores of size 20 to 260 nm and 60 to 260 nm, respectively (Fig. 3, *a*). The average size of crystallites was 150 nm, of pores – 130 nm. The shape of crystallites and pores was near-spherical. With a larger magnification 100000× and 200000× the structure morphology had a similar appearance (Fig. 3, *b*, *c*). However, there were finer nanocrystals of size about 10 nm. Fine nanocrystals were grouped into coarser ones of size 50 to 80 nm, 100 to 130 nm and 300 nm. The largest pores had the size about 1 μm (Fig. 3, *d*).

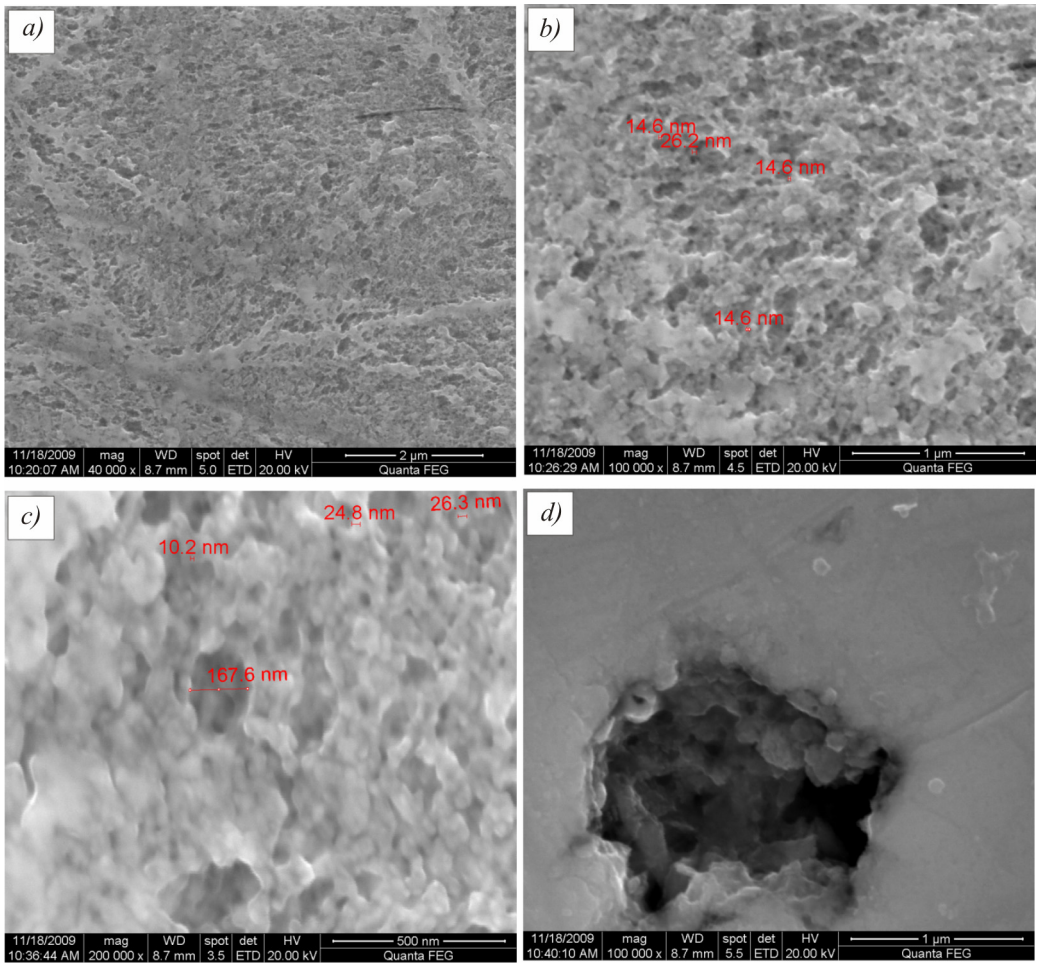

Fig. 3. The pictures of microstructure morphology of p-type thermoelectric material $(Bi_2Te_3)_x$-$(Sb_2Te_3)_{1-x}$ ($x \approx 0.26$ mol.%) obtained by scanning electron microscope.

The situation was different in *n*-type samples (Fig. 4). The microstructure was made as fiber bundles oriented relative each other at different angles (Fig. 4, *a*). The fiber bundles were rolled at the angles of 120° – 180°, and at their bend points there were voids from 1 to 5 μm. The transverse size of the fibers was close to 40 μm (Fig. 4, *b*). Thin fibers were combined into larger fibers several μm thick and several tens of μm long. At larger magnification it is seen that the fibers consist of fine nanocrystals of size 8 to 30 nm (Fig. 4, *c*, *d*). Apart from the fibers, nanocrystals formed coarser crystals of average size 60 nm, 120 nm and 300 nm. However, pores in *n*-type samples were of larger size than in *p*-type samples.

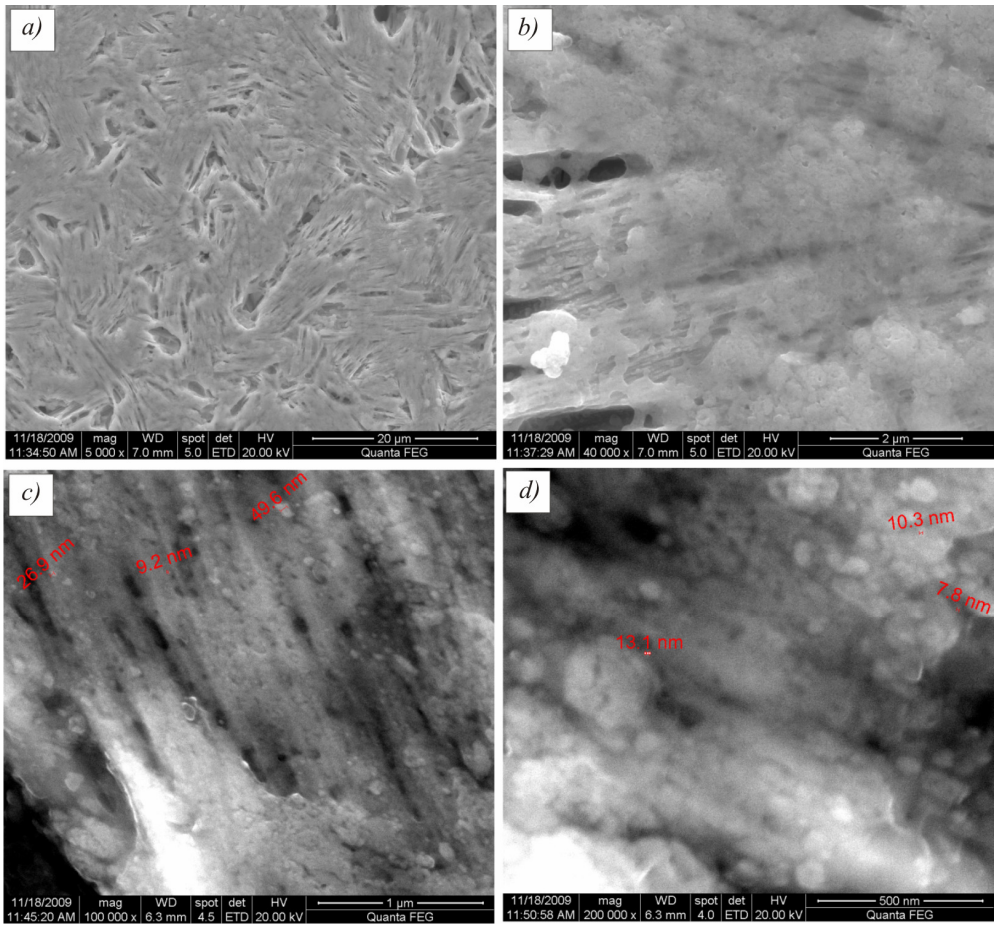

Fig. 4. Pictures of microstructure morphology of n-type thermoelectric material $(Bi_2Se_3)_x$-$(Bi_2Te_3)_{1-x}$ ($x \approx 0.06$ mol.%) obtained by scanning electron microscope.

The thermoelectric figure of merit of nanostructured thermoelectric materials was determined by the method of separate measurement of thermoEMF, electric resistivity and thermal conductivity. The electric resistivity was measured under isothermal conditions, and thermoEMF – at temperature gradient along the sample about 1 K/cm. The thermal conductivity was measured under transverse adiabatic conditions with temperature gradient along the sample 0.5 K/cm, and carrier concentration – by means of the Hall effect in a magnetic field with the induction of 0.24 T. The measured results are given in Table 1.

Table 1

Thermoelectric properties of extruded materials

Parameters	$(Bi_2Te_3)_x$-$(Sb_2Te_3)_{1-x}$ *p*-type	$(Bi_2Se_3)_x$-$(Bi_2Te_3)_{1-x}$ *n*-type
ThermoEMF, α, μV/K	224	225
Electric resistivity, $\sigma \times 10^{-5}$, Ω·m	0.95	1.06
Thermal conductivity *k*, W/(m·K)	1.6	1.7
Thermoelectric figure of merit $Z \times 10^{-3}$, K^{-1}	3.3	2.8
Charge carrier mobility, $\mu_n \times 10^4$, $cm^2/V{\cdot}s$	2.7	1.5
Charge carrier concentration $n \times 10^{18}$, cm^{-3}	2.2	4.0

These research results have shown that samples orientation relative to ingot axis produced no effect on the measured parameter values, unlike the results of [9]. This can be due to the difference in material production technologies and their structure. It is noteworthy that thermoelectric figure of merit of *n*-type nanostructured material is lower than that of *p*-type material. Moreover, lower carrier mobility and large concentration contribute to electric resistivity and thermal conductivity increase, though slight, but reducing the thermoelectric figure of merit of this solid solution by 15 %. Comparing the microstructure patterns of investigated materials, it can be noted that the reduction of thermoelectric figure of merit and carrier mobility in *n*-type nanostructured material is probably affected by the fibrous structure randomly oriented in space and the presence of large pores of size up to 5 μm.

3. Conversion factor measurement

3.1. Method with two copper plates

Conversion factor of thermoelectric module was calculated using the method with two copper plates with regard to experimental data as follows. For this purpose, the equations describing thermoelectric processes in thermoelectric modules were employed. Under thermal equilibrium the heat of the Peltier effect and half the Joule heat of thermoelectric module are equal to heat flow from the hot to cold side of the device [10]. This thermal equilibrium corresponds to constant heat flow at maximum temperature difference ($T_h - T_c$) and can be described as

$$\alpha_m \cdot T_h \cdot I + 0.5 \cdot R_m \cdot I^2 - k_m \cdot (T_h - T_c) = 0, \quad (1)$$

where α_m is thermoEMF of thermoelectric module; T_h is hot side temperature of thermoelectric module; T_c is cold side temperature of thermoelectric module; I is electric current flowing through thermoelectric module; R_m is electric resistance of thermoelectric module; k_m is thermal conductivity of thermoelectric module.

Voltage U on thermoelectric module can be calculated from the equality [9]

$$U = \alpha_m \cdot (T_h - T_c) + I \cdot R_m, \quad (2)$$

where α_m, k_m, R_m depend on temperatures T_h and T_c. These dependences can be described by equations

$$\alpha_m = \alpha_1 + \alpha_2 \cdot T + \alpha_3 \cdot T^2 \quad T_h - T_c = 0; \quad (3)$$

$$\alpha_m = (\alpha_m(T_h) - \alpha_m(T_c)) / (T_h - T_c) \quad T_h - T_c \neq 0; \quad (4)$$

$$R_m = R_1 + R_2 \cdot T + R_3 \cdot T^2 \quad T_h - T_c = 0; \quad (5)$$

$$R_m = (R_m(T_h) - R_m(T_c)) / (T_h - T_c) \quad T_h - T_c \neq 0; \quad (6)$$

$$k_m = k_1 + k_2 \cdot T + k_3 \cdot T^2 \quad T_h - T_c = 0; \quad (7)$$

$$k_m = (k_m(T_h) - k_m(T_c)) / (T_h - T_c) \quad T_h - T_c \neq 0. \quad (8)$$

Solution of Eq. (1) and (2), together with Eq.(3 – 8) allows determination of α_m, R_m, and k_m from the series of experiments performed. During each experiment, $\Delta T_{\max}$ was measured at constant T_h and a variation of voltage and current. The resulting values made it possible to determine α_m, R_m, and k_m with an error less than 3 %.

Heat N_h, transferred by thermoelectric module was calculated according to equation (1) under equilibrium conditions. Conversion factor of thermoelectric module η was determined as [2, 11]

$$\eta = \frac{N_h}{U \cdot I}. \quad (9)$$

The values of conversion factor at cold surface temperatures $T_c = 273$ K and $T_c = 323$ K in the first experiment are represented in Figs. 5 and 6.

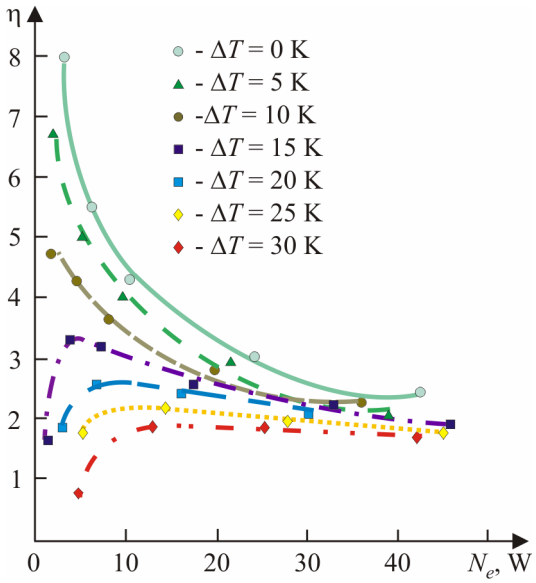

Fig. 5. Conversion factor η *versus electric power* N_e *at temperature* T_c *= 273 K.*

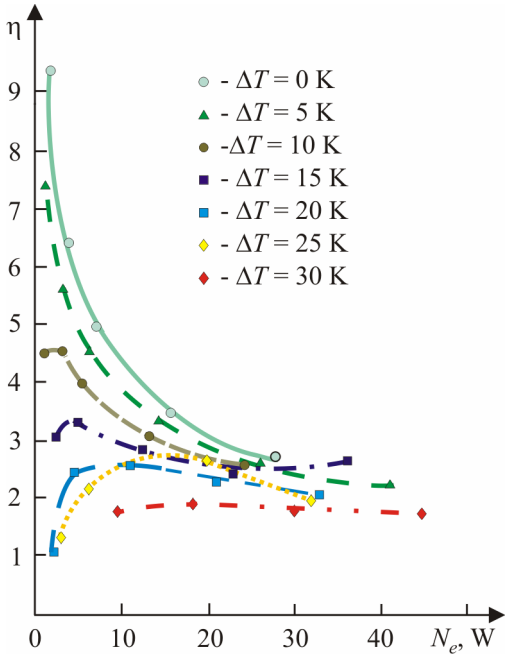

Fig. 6. Conversion factor η *versus electric power* N_e *at temperature* T_c *= 323K.*

There was conversion factor reduction with increase in power and temperature difference for given values of T_c. For $T_c = 323$ K conversion factor increased with temperature difference up to 10 K. Maximum value of conversion factor $\eta = 9.3$ was at consumed electric power $N_e = 2$ W and $\Delta T = 0$. Minimum value of conversion factor was 1.8 at $N_e = 40$ W and $\Delta T = 30°$.

3.2. Method with one copper plate and a heater

In this method, heat transferred by thermoelectric module to copper plate was determined at its temperature rise within 10 s. This time period of temperature variation was much in excess of the time of heat propagation in copper plate ($t << 1$ s). The quantity of heat transferred to copper plate N_h was

calculated by relationship [12]:

$$N_h = \frac{cm(T_2 - T_1)}{t}, \tag{10}$$

where c is copper heat capacity; m is copper plate mass; T_1 and T_2 are copper plate temperatures during the first and tenth seconds of measurement. Conversion factor in the second method was calculated according to Eq. (9).

During the second experiment, conversion factor was measured for three electric power values of thermoelectric module. The energy transferred to copper plate was measured and calculated according to Eq. (10) and used for the calculation of conversion factor according to Eq. (9). The measured results for temperature range of +17 °C to +45 °C are represented in Fig. 7. The minimum and maximum thermal power was reduced from 5 W to 4.8 W and from 21.6 W to 14.1 W at consumed electric power from $N_e = 0.75$ W to $N_e = 7.6$ W, respectively. Temperature difference ΔT between the hot and cold surfaces of thermoelectric module varied from 4 to 18 degrees. Conversion factor of this thermomodule reached 8. One should note sufficiently good agreement between the results of measurement of thermomodule conversion factor by both methods.

However, thermoelectric materials used for the manufacture of thermoelectric modules, had thermoelectric figure of merit $ZT \approx 1$ at room temperature. During these experiments we employed thermoelectric nanomaterials with nanocrystallite size 8 to 30 nm. Nanostructured solid solutions $(Bi_2Te_3)_x$-$(Sb_2Te_3)_{1-x}$ of p-type possess higher thermoelectric figure of merit as compared to n-type material. Therefore, one of the ways for increasing the operating efficiency of thermoelectric modules is to improve the thermoelectric figure of merit of n-type $(Bi_2Se_3)_x$-$(Bi_2Te_3)_{1-x}$ solid solutions. The results of research point to the following possibilities for improving the efficiency of nanostructured thermoelectric modules.

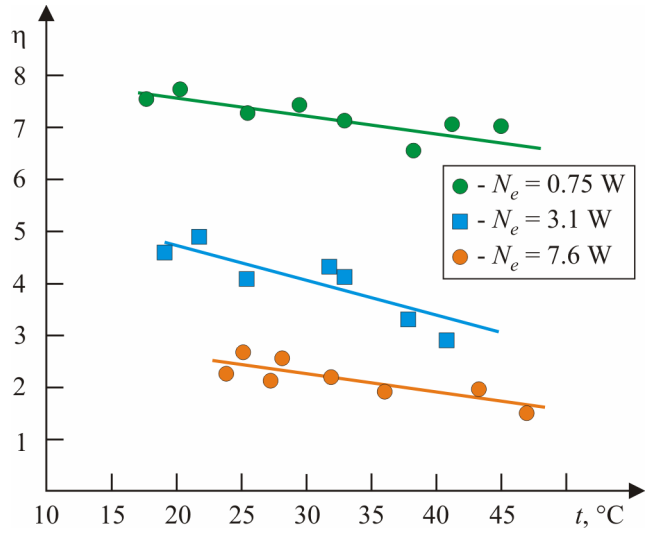

Fig. 7. Conversion factor versus temperature T_h for three values of electric power N_e.

First, apart from the known method of thermal conductivity reduction due to size reduction of nanocrystallites to nanometer units [7, 13, 14], good promise is shown by the development of extrusion method process conditions with a view to improve structural perfection of materials. In our opinion, size reduction of pores and orientation of fibers in n-type nanomaterial, structured in a particular direction, can assure figure of merit increase. Second, doping of solid solutions with a view to improve the thermoelectric properties and the effect of nanostructured materials on structural perfection.

Conclusions

The microstructure morphology of extruded ingots of *p*- and *n*-type thermoelectric materials based on solid solutions of bismuth and antimony chalcogenides was studied. The extruded thermoelectric materials had nanocrystalline structure. Nanocrystals in *p*-type samples were of spherical shape of size 8 to 30 nm combined into clusters of size 60 to 300 nm. Between crystallites there were pores as big as 1 μm. Nanocrystals in *n*-type samples were of similar spherical shape and dimensions, but formed fibers 30 to 60 nm thick. The fibers were combined into bundles of length up to several tens of μm with different orientation and bend by 120 to 180° where the pores of size 1 to 5 μm were observed. Apart from the fibers, nanocrystals formed coarser crystallites of the average size 60 nm, 120 nm and 300 nm.

Using the method of separate measurement of thermoEMF, electric resistivity and thermal conductivity it was established that the thermoelectric figure of merit of extruded nanocrystalline *p*-type materials is $Z = 3.3 \times 10^{-3}$ K^{-1}, and of *n*-type – $Z = 2.8 \times 10^{-3}$ K^{-1}.

The lower figure of merit of *n*-type material can be due to lower mobility and high carrier concentration than in *p*-type material.

The conversion factor of thermoelectric modules made of extruded telluride solid solutions was measured. For this purpose, two measurement methods were developed. In the first method, equations describing thermoelectric processes in thermomodules were used for the calculation of thermoelectric and electric parameters, namely thermoEMF, thermal conductivity, as well as electric current, electric resistance and voltage on thermoelectric modules. In the second method, conversion factor was measured under thermoelectric modules operation as heat pumps. These methods showed high efficiency of thermoelectric modules for heat transfer in the temperature range of +17 to +45 °C. Maximum conversion factor reached 6.8 to 8.2 for heat transfer at electric power 0.75 to 2 W and temperature difference 4 – 5 degrees. However, increase in electric power to 40 W and temperature difference to 30° reduced conversion factor to 1.8.

These results demonstrated the possibility of using thermoelectric modules for heating, as well as the necessity of increasing the efficiency of thermoelectric materials. The thermoelectric efficiency of thermoelectric materials can be increased considerably due to size reduction of nanocrystals to nanometer units, improvement of structure perfection and doping of extruded nanothermoelectric materials. Compactness, noiselessness and high efficiency with account of using new nanotechnologies will contribute to a wider application of thermoelectric power converters in new heating systems.

Acknowledgement. The Authors express their gratitude to Dr. A.Churilov for the helpful discussion.

References

1. S.W. Angrist, Direct Energy Conversion, 3d ed. (Boston, Allyn and Bacon Inc., 1976), 518p.
2. D.M. Rowe, CRC Handbook of Thermoelectrics (Boca Raton, CRC Press, 2010), 701p.
3. A.J. Mortlock, Simplified Experiment Demonstrating Interstitial Diffusion in Alpha Iron, *Am. J. Phys.* **33**, 1033 – 1035 (1965).
4. S.B. Riffat, X. Ma, Thermoelectrics: a Review of Present and Potential Applications, *Appl. Therm. Eng*. **23**, 913 – 935 (2003).
5. L. Chen, J. Li, and F.J. Sun, Heat Transfer Effect on Optimal Performance of Two-Stage Thermoelectric Heat Pumps, *Journal of Mechanical Engineering Science* **221**, 1635 – 1641 (2007).
6. B.C. Sales, Smaller Is Cooler, *Science* **295**, 1248 – 1249 (2002).

7. A. Majumdar, Thermoelectricity in Semiconductor Nanostructures, *Science* **303**, 777 – 778 (2004).
8. Q. Zhang, Q. Zhanga, S. Chen, W. Liu, K. Lukas, X. Yan, X. Wang, D. Wang, C. Opeil, G. Chen, and Z. Ren, Suppression of Grain Growth by Additive in Nanostructured *p*-type Bismuth Antimony Tellurides, *Nano Energy* **1**, 183 – 189 (2012).
9. I.A. Drabkin, V.B. Osvensky, and Yu.N. Parkhomenko, Anisotropy of Thermoelectric Properties of *p*-Type Thermoelectric Material Based on $(Bi, Sb)_2Te_3$, *J.Thermoelectricity* **3**, 37 – 49 (2013).
10. Thermoelectric Technical Reference – Mathematical Modeling of TEC Modules. *FerroTec*.: http://www.ferrotec.com (2009).
11. A.F. Ioffe, *Semiconductor Thermoelements and Thermoelectric Cooling* (London: Infosearch, 1957), 188p.
12. T.I.Tofimova, *Course of Physics* (Moscow: Vyschaya Shkola, 1990), 478 p.
13. M.S. Dresselhaus, G. Chen, M.Y. Tang, R. Yang, H. Lee, D. Wang, Z. Ren, J.P. Fleurial, and P. Gogna, New Directions for Low-Dimensional Thermoelectric Materials, *Adv. Mater*. **19**, 1043 – 1053 (2007).
14. L.P. Bulat, D.A. Kossakovski, and D.A. Pshenai-Severin, Effect of Phonon Thermal Conductivity on Thermoelectric Figure of Merit of Bulk Nanostructured Materials with Tunneling Contacts, *J.Thermoelectricity* 2, 37 – 44 (2013).

Submitted 09.04.2013.